

Cite this article as: Zhang Ning, Meng Li, Zhang Xing, et al. Crystallographic Behavior of Deformed Grains in Cold-Rolled HCP Alloy (CP-Ti) Using Experiment and Simulation by Reaction Stress Model[J]. Rare Metal Materials and Engineering, 2022, 51(04): 1158-1163.

ARTICLE

Crystallographic Behavior of Deformed Grains in Cold-Rolled HCP Alloy (CP-Ti) Using Experiment and Simulation by Reaction Stress Model

Zhang Ning¹, Meng Li¹, Zhang Xing², Zhang Wenkang³, Zhong Sheng⁴, Mao Weimin²

¹Metallurgical Technology Institute, Central Iron and Steel Research Institute, Beijing 100081, China; ²School of Materials Science and Engineering, University of Science and Technology Beijing, Beijing 100083, China; ³Technology Centre of Shanxi Taigang Stainless Steel Co., Ltd, Taiyuan 030003, China; ⁴ABB Corporate Research Center, North Carolina 27606, USA

Abstract: After commercially pure titanium (CP-Ti) annealed sheet was cold-rolled to 9% reduction, electron backscatter diffraction (EBSD) and scanning electron microscopy (SEM) were employed to evaluate activated slip and twin in the samples. Meanwhile, the activation of slip systems in deformed grains and the interaction between grains were simulated by reaction stress (RS) model, in which the plastic deformation process in a grain was regarded as a combined consequence of external stress and statistically varied intergranular reaction stress. The results indicate that the reaction stress model is suitable to estimate the deformation behavior of polycrystalline titanium. The model predicts slip occurring in deformed titanium grains, which is confirmed by experimental data. The distribution of slip and twin in deformed grains is non-uniform, connecting to uneven in-grain strain distribution. This uneven in-grain strain can also be generated by deformation of adjacent grains with different crystal orientations. When the plastic deformation in a grain shows significant difference from that of its neighboring grain, additional local slips are triggered to decrease the strain inconsistency. The plastic strain is realized by mechanical twinning in some cases, which combines with the active slips to satisfy in-grain and intergranular strain consistency.

Key words: titanium; slip; twinning; simulation; reaction stress (RS) model; inhomogeneous strain distribution

Compared to other polycrystalline metals and alloys, polycrystalline titanium (Ti) is known to have a complicated mechanism for polycrystalline plastic deformation, and it involves multiple deformation mechanisms, including basal slip ($\{0001\} \langle \bar{2}110 \rangle$), prismatic slip ($\{1\bar{1}00\} \langle 1\bar{1}20 \rangle$), various pyramidal slips ($\{10\bar{1}1\} \langle 1\bar{2}10 \rangle$, $\{10\bar{1}1\} \langle 11\bar{2}3 \rangle$, etc), and mechanical twinning^[1-5]. The complexity of titanium plastic deformation makes it difficult to predict and estimate the evolution of microstructure and texture in deformed titanium sheets. Various models are proposed to study crystallographic plastic deformation, including advanced lamel (ALAMEL), grain interaction (GIA), and visco-plastic self-consistent (VPSC) models. These models originate from Taylor principle, which states identical strain tensor in every grain, and different modification or relaxation will be adopted

according to specific conditions^[6-10]. This causes problem for deformation prediction. In order to maintain a uniform strain required for Taylor principle, the type and number of slip systems to be activated have to be determined for each individual grain in the aggregate. In addition, although Taylor principle has been adopted in wide applications, it has limitation in explaining stress incompatibility in the grains. That is, continuous strain in polycrystals can be actualized, while stress may be inconsistent or may not conform to the stress in a real situation.

Reaction stress (RS) model states that the grains deform under the combination of external load and intergranular reaction stress. At the beginning, plastic deformation is triggered by external loading, and then intergranular reaction stress takes part in the following deformation process in

Received date: April 24, 2021

Foundation item: National Key Research and Development Program of China (2017YFB0903901); China Shanxi Provincial Science and Technology Major Special Project (20191102004); National Natural Science Foundation of China (51571024)

Corresponding author: Meng Li, Ph. D., Senior Engineer, Metallurgical Technology Institute, Central Iron and Steel Research Institute, Beijing 100081, P. R. China, Tel: 0086-10-62187014, E-mail: mengli@cisri.com.cn

Copyright © 2022, Northwest Institute for Nonferrous Metal Research. Published by Science Press. All rights reserved.

consideration of statistical environment. Based on the consideration of intergranular stress and strain consistence, the activation of slip system and crystal orientation transition during deformation can be analyzed by RS model^[11-14]. This model has been proven to be effective in simulating deformation texture evolution of bcc and fcc metals and their alloys. More to the point, RS model does not regard crystal grain as an isolated individual but part of a group of grains, and thus any actions and deformations are the coordination of all the grains in the system. RS model uses a statistical method to predict the crystallographic deformation and activation of slip system, and considers the slip system activation in a sequential fashion. The deformation should start with a single slip system under the external loading, and then the reaction stress is accumulated with the deformation. As soon as the stress accumulation exceeds the required stress level, another slip system will be activated. This stress accumulation→new slip activation→stress accumulation cycle will repeat until the required strain is realized.

In RS model, both stress and strain consistency are considered and strain continuity is achieved via coordination of plastic and elastic strains in the matrix^[11-14]. For polycrystals, strain fluctuates both inside a deformed grain and across the grain boundaries, meaning that the strain distribution is inhomogeneous^[15]. This factor complicates the theoretical analysis for polycrystal metals and alloys and makes it difficult to predict texture evolution and orientation changes during deformation. This study investigated plastic deformation behavior of deformed grains in a polycrystalline titanium using RS model. The inhomogeneous strain distribution as well as its cause and influence on the deformation process were analyzed. The aim is to clarify the mechanism of crystallographic plastic deformation of polycrystalline titanium.

1 Experiment

A 40 mm×25 mm×5 mm sample was cut from an as-forged TA2-grade titanium (0.1wt% C, 0.05wt% N, 0.015wt% H, 0.025wt% O, 0.3wt% Fe, 0.4wt% others, and the balance Ti). The sample was annealed at 800 °C for 2 h under Ar

atmosphere. The initial microstructure and orientations of selected grains were measured in the lateral plane with scanning electron microscope (SEM) and electron backscatter diffraction (EBSD) techniques, and the analysis indicated an average annealed grain size of ~200 μm. Then the sample was cold rolled to 9% reduction. After deformation, the grains were characterized by SEM and EBSD to trace and evaluate the orientation change as well as microstructure evolution after rolling deformation.

2 Results and Discussion

2.1 Experimental results

Fig. 1 shows a grain marked with * and its surrounding grains labeled as No. 1~11 before (Fig. 1a) and after (Fig. 1b) the rolling deformation. The band contrast maps were measured via EBSD, in which plastic strain generated by rolling can be identified. The measured deformed grains are compared to those simulated grain shapes, as depicted in Fig. 1c. The solid lines correspond to real grain boundaries after deformation and the dotted lines show the calculated grain boundaries. In simulation, homogeneous strain in the grains follows the Taylor principle. The obvious shape difference among measured and simulated grain boundaries indicates that the Taylor principle does not capture the complexity in titanium deformation and the inhomogeneous strain distribution.

The microstructures before and after rolling were measured by SEM, and the results are shown in Fig. 2. Based on the measured crystal orientation of grain * and the slip and twinning traces shown in Fig. 2b, all the activated penetrating slip systems and local slip systems were identified and simulated, and the results are listed in Table 1. RS model was used for calculation and its validity has been demonstrated and confirmed in our previous works^[11-14]. Rolling reduction of 9% corresponds to the true strain of -0.094, and the simulation step was set as -0.001, so the overall steps in calculation were 94. The occurrence area of twinning approximately occupies 5% of the deformed grain *, and it demands a special simulation step and will be discussed separately in the following sections.

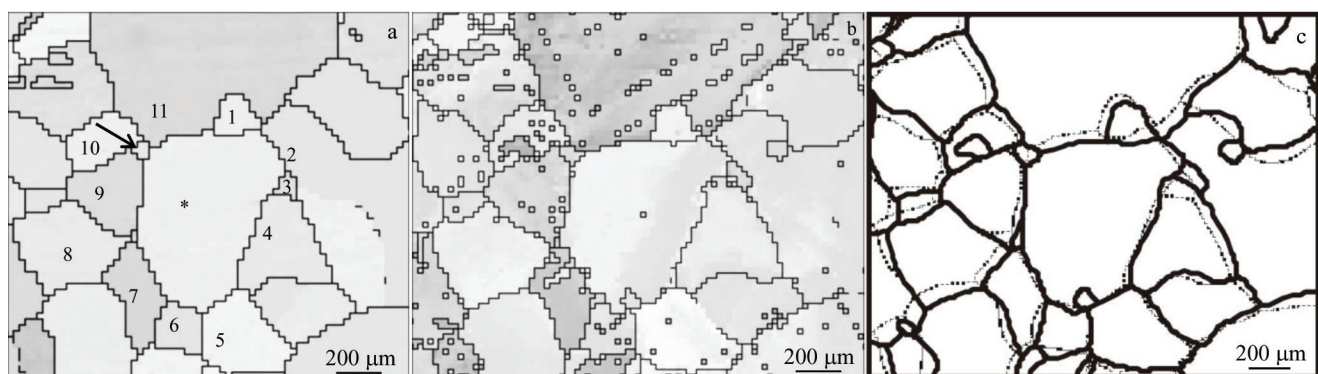


Fig.1 EBSD band contrast maps before (a) and after (b) 9% rolling reduction and comparison of real shapes (solid lines) and simulated shapes (dotted lines) (c)

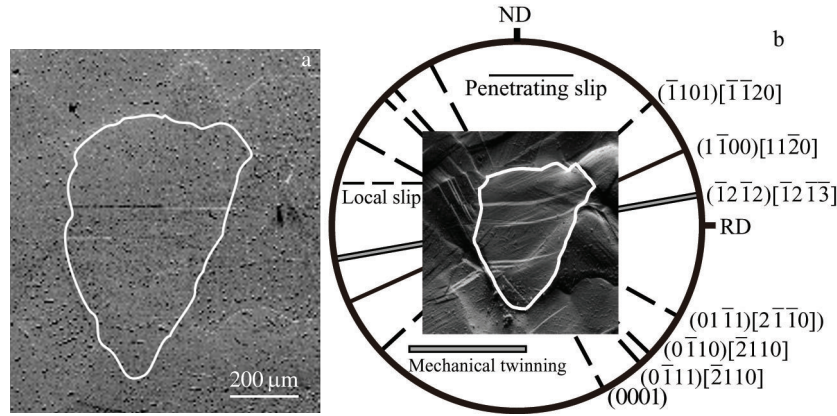


Fig.2 Activated slips and mechanical twinning of grain * marked in Fig.1a during deformation: (a) SEM image of initial microstructure and (b) slip and twinning traces and corresponding slip/twinning systems

Table 1 Activated slip systems of grain * shown in Fig.1a and calculated with RS model

Mode	Activated slip system	Occurrence location in experiment marked in Fig.2	Accumulation step in calculation
Slip	(1 $\bar{1}$ 00) [11 $\bar{2}$ 0]	Penetrating grain *	22
Slip	(0 $\bar{1}$ 10) [$\bar{2}$ 110]	Lower left region	20
Slip	(01 $\bar{1}$ 1) [2 $\bar{1}\bar{1}$ 0]	Upper right region	2
Slip	(0 $\bar{1}$ 11) [$\bar{2}$ 110]	Scatter in the middle	48
Slip	(0001) [$\bar{2}$ 110]	Local in the middle	2
Slip	($\bar{1}$ 101) [$\bar{1}\bar{1}$ 20]	Right middle	0

2.2 Interaction between deformed grains

RS model is selected to analyze the deformation process of polycrystalline titanium because of its ability to address complex deformation process that is intrinsic in polycrystalline titanium metal. RS model considers that the grain deformation is due to the combination of external stress and intergranular interaction, and in simulation, the intergranular strain and stress continuity are maintained via a natural way^[14]. During the rolling deformation, the stress tensor $[\sigma_{ij}]$ that a deformed grain undergoes can be illustrated as^[12]:

$$[\sigma_{ij}] = \sigma_y \begin{bmatrix} \frac{1}{2} & 0 & 0 \\ 0 & 0 & 0 \\ 0 & 0 & -\frac{1}{2} \end{bmatrix} + \sigma_y \begin{bmatrix} 0 & -\mu\epsilon_{12}\frac{d}{b} & -\mu\epsilon_{13}\frac{d}{b} \\ -\mu\epsilon_{21}\frac{d}{b} & 0 & -\mu\epsilon_{23}\frac{d}{b} \\ -\mu\epsilon_{31}\frac{d}{b} & -\mu\epsilon_{32}\frac{d}{b} & 0 \end{bmatrix} \quad (1)$$

In Eq.(1), subscripts 1, 2, 3 represent rolling direction (RD), transverse direction (TD), and normal direction (ND) of the rolled sheet, respectively; σ_y is the macroscopic flow yield stress during rolling; μ is the generalized Schmid factor of the activated slip system; $\epsilon_{ij|i \neq j}$ is the plastic strain induced by active slip; d is the dislocation distance, and b is the length of Burgers vector. The first term of Eq. (1) corresponds to the external stress applied on the sheet, and the second term corresponds to the intergranular elastic reaction stress^[12]. Under the stress tensor expressed in Eq. (1), the slip system will be activated when its Schmid factor μ is the highest among all slip systems, leading to the gradual changes in

crystal orientation. As soon as the grain orientation starts to change, the Schmid factors of the slip systems will change too, and thus the system with the new highest factor will be triggered subsequently. Every slip movement will cause interaction among neighboring grains, leading to the variation in the second term in Eq.(1). Apparently, activation of a slip system is not an isolated event but will cause changes in the reaction stress value accordingly and in turn will determine subsequent slip system to be activated and ultimately the change route for grain orientation^[11-13].

Reaction stress will allow the strain to increase but within a limit, and thus the values of σ_{ij} should have an upper-limit. As soon as σ_{ij} reaches the arbitrary upper-limit, it indicates that the stress accumulated in adjacent grains may reach their yield point, leading to local slips, which generally occur close to the grain boundaries. As the slip system is switched, the reaction stress may reduce. The upper-limits $[\sigma_{ij}]_{lim}$ can be represented by Eq.(2)^[11-13]:

$$[\sigma_{ij}]_{lim} = \begin{bmatrix} \sigma_{11} \equiv \sigma_y/2 & |\sigma_{12}| \leq \alpha_{12}\sigma_y/2 & |\sigma_{13}| \leq \alpha_{31}\sigma_y/2 \\ |\sigma_{21}| \leq \alpha_{12}\sigma_y/2 & \sigma_{22} \equiv 0 & |\sigma_{23}| \leq \alpha_{23}\sigma_y/2 \\ |\sigma_{31}| \leq \alpha_{31}\sigma_y/2 & |\sigma_{32}| \leq \alpha_{23}\sigma_y/2 & \sigma_{33} \equiv -\sigma_y/2 \end{bmatrix} \quad (2)$$

where α is the effective coefficients of the maximal reaction stresses, within the range of 0~1. $\alpha_{ij} \equiv 0$ means that no reaction stress is considered, similar to the single crystal state defined by Sachs model^[16]; whereas $\alpha_{ij} \equiv 1$ represents the theoretically highest reaction shear stress^[12]. The shear modulus of pure titanium at room temperature is 44 GPa, and the ultimate yield

σ_y is 373 MPa^[10]. So, the upper limit of elastic shear strain is calculated as $\pm 8.48\%$.

To simulate the grain orientation evolution of deformed titanium, several types of slip systems, including $\{0001\} \langle \bar{2}110 \rangle$, $\{1\bar{1}00\} \langle 11\bar{2}0 \rangle$, $\{10\bar{1}1\} \langle 1\bar{2}10 \rangle$ and $\{11\bar{2}2\} \langle 11\bar{2}\bar{3} \rangle$ systems, are considered, and the corresponding critical resolved shear stresses are 1.5: 1: 1.3: 1.3^[17]. When a free singular grain is considered, α_{ij} is set as 0 since there is no interaction among grains. Under this condition, only $(0\bar{1}10) [\bar{2}110]$ slip system is activated in 94-step simulation. The ultimate shear strains are accumulated to $\varepsilon_{12} = -0.0431$, $\varepsilon_{31} = -0.0348$ and $\varepsilon_{23} = -0.0111$. Since all the resultant strains exceed the supposed upper-limit of elastic strain, the assumption that deformation occurs in an isolated grain without affecting neighboring grains is not realistic and should be revised. By applying RS model, the calculated shear strains are $\varepsilon_{12} = -0.0009$, $\varepsilon_{31} = -0.0015$ and $\varepsilon_{23} = -0.0025$, so all the strains fall into the elastic strain range. The accumulation and evolution of ε_{ij} in every direction of grain * are plotted in Fig.3. It is worth noting that all values are within the elastic limit. At every strain peak in Fig.3, a new slip system is activated. The frequent changes of activated slip systems are greatly influenced by the second term in Eq.(1), namely, the reaction stress term $[\sigma'_{ij}]$. As soon as the stress is accumulated to the threshold, a corresponding slip system will be triggered, resulting in the reduction in the strain and thus maintaining the continuity of the intergranular strain and stress.

Similarly, the active slip systems and their respective simulation steps are listed in Table 1. Except $(\bar{1}101) [\bar{1}\bar{1}20]$ slip system, all other observed slips have been predicted in the simulation, as shown in Table 1. This proves that the reaction stress model is effective and valid to theoretically analyze the rolling deformation process of polycrystalline titanium.

2.3 Inhomogeneous strain distribution

All slip systems, whether activated or not, are under stress during deformation, and the only difference is that the stress applied on an active slip system has surpassed its activation stress limit. At the same time, the Schmid factor of the inactivated slip systems may be slightly lower than that of the active slip system. Due to the combination of external load

and reaction stress by surrounding matrix, additional slip may be easily stimulated in local areas inside grains, or near grain boundaries. The local slip shown in Fig.2 can be connected to locally uneven strain distribution.

In order to clarify the deformation behavior of grain * as its surrounding grains are deformed, the generated shear stress ε_{31} of surrounding grains No. 1~11 are calculated using RS model when the same α_{ij} are used in the calculation. The results are summarized in Table 2. The surrounding grains are divided into 2 groups, namely, upper left group (grain 1, 8, 9, 10, 11) and lower right group (grain 3, 4, 5, 6). The length of the grain boundaries between grain * and the grains in these two groups are measured. Then the total grain boundaries in each grain group are measured and its total boundary length is recorded. The grain boundary shared between grain groups and grain * is divided by its corresponding total boundary length, which is considered as a weighting coefficient used for calculating $\Sigma \varepsilon_{31}$. As shown in Table 2, the $\Sigma \varepsilon_{31}$ values of upper left group and lower right group are 0.003 04 and -0.003 24, respectively, and the ε_{31} of grain * is equal to -0.0015.

The schematic in Fig. 4 illustrates the shear stress $\Sigma \varepsilon_{31}$ applied on the grain * through the combined effect of upper left and lower right grain groups before and after the deformation. Based on the calculation, similar ε_{31} shear values are produced by these two groups but in opposite directions, and thus the outcome is that these two forces have canceled each other to a large extent. The corresponding strains, on the other hand, can be easily realized during deformation. However, since the grain * is surrounded by the polycrystalline matrix, its ε_{31} will be transferred to neighboring grains and its effect cannot be ignored. In particular, the ε_{31} of grain * and upper left group are in opposite direction, causing discontinuity in local stress and strain. This phenomenon is possibly responsible for the local activation of $(\bar{1}101) [\bar{1}\bar{1}20]$ slip in grain * (Fig.2c, Table 1), which helps to reduce the local stress and strain inconsistency. This slip system is not represented in RS model but its occurrence causes local plastic deformation and thus re-balances stresses in the matrix, contributing to the compatibility of strain and stress among grains.

The calculation confirms that only $\{2\bar{1}\bar{1}2\} \langle 2\bar{1}\bar{1}3 \rangle$ twinning systems which includes six components are able to move. The Schmid factors and ε_{ij} of each system are shown in Table 3. Interestingly, the active twinning system $\{\bar{1}2\bar{1}2\} \langle \bar{1}2\bar{1}\bar{3} \rangle$ observed in Fig.2 actually does not have the highest Schmid factor among all discussed slip systems. This phenomenon can be attributed to the strain incompatibility induced by different twinning systems. A slip with high strain usually leads to high inconsistency and thus is less likely to be tolerated in the matrix. Compared with other twinning systems, the strain values of $\{\bar{1}2\bar{1}2\} \langle \bar{1}2\bar{1}\bar{3} \rangle$ twinning system are $\varepsilon_{12} = -0.0129$, $\varepsilon_{13} = -0.0248$ and $\varepsilon_{23} = 0.0082$, each of which is relatively low. Thus, the activation of $\{\bar{1}2\bar{1}2\} \langle \bar{1}2\bar{1}\bar{3} \rangle$ twinning system will be more compatible with the matrix. In grain *, the calculated slip strain by RS model is shown to be $\varepsilon_{13} = -0.0015$ and $\varepsilon_{23} = -0.0025$, which can be compensated by the $\varepsilon_{13} = 0.0248$ and $\varepsilon_{23} =$

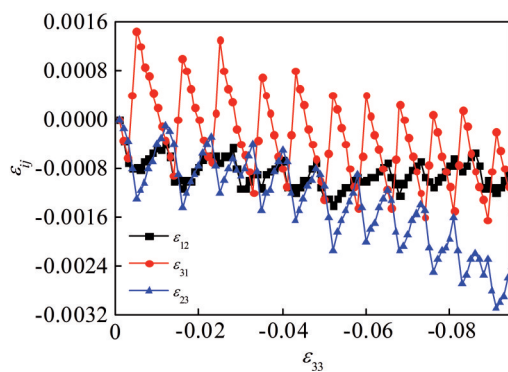


Fig.3 Accumulation and evolution of ε_{ij} in every direction of grain *, calculated based on RS model

Table 2 Calculated ϵ_{31} of the grains in Fig.1 after rolling deformation

Grain No.	Orientation angle/(°)			ϵ_{31} calculated by RS model	Percentage of grain boundary length (upper left group)	Percentage of grain boundary length (lower right group)
	ϕ_1	Φ	ϕ_2			
*	164	102	351	-0.001 5	1	1
1	164	98	317	0.000 6	0.239	
2	144	83	297	-0.001 1		
3	144	41	261	-0.007 4		0.137
4	136	56	246	0.0		0.463
5	3	63	41	-0.01		0.221
6	20	56	2	-0.000 1		0.179
7	153	23	231	-0.000 7		
8	97	99	273	-0.001	0.057	
9	148	57	273	-0.000 8	0.307	
10	141	44	284	-0.005 3	0.068	
11	89	154	321	0.010 8	0.329	
Weighted $\Sigma\epsilon_{31}$					0.003 04	-0.003 24

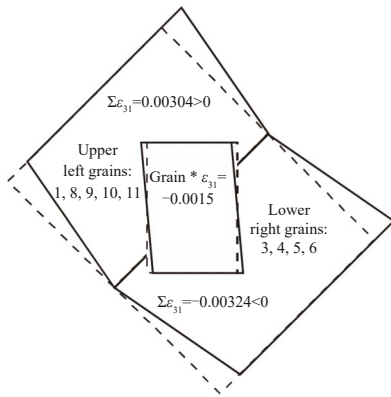


Fig.4 Schematic of ϵ_{31} difference applied on grain * by surrounding grains before (full line) and after (dotted line) deformation

0.0082 of $\{ \bar{1}2\bar{1}2 \} < \bar{1}2\bar{1}\bar{3} >$ twinning without aggravating the strain inconsistency in the system. Therefore the activation of $\{ \bar{1}2\bar{1}2 \} < \bar{1}2\bar{1}\bar{3} >$ twinning system is preferred. In other words, similar to the situation of local slip, the activation of twinning also needs to consider the total effect of strain consistency caused by the twinning.

Table 3 Possible $\{ 2\bar{1}\bar{1}2 \} < 2\bar{1}\bar{1}\bar{3} >$ twinning systems and the corresponding ϵ_{ij}

Grain No.	Twinning system	Schmid factor	ϵ_{12}	ϵ_{13}	ϵ_{23}
1	$(2\bar{1}\bar{1}2)[2\bar{1}\bar{1}\bar{3}]$	0.435 4	-0.033 3	-0.012 5	0.040 2
2	$(11\bar{2}2)[11\bar{2}\bar{3}]$	0.395 6	0.051 7	0.013 4	0.022 4
3	$(\bar{2}112)[\bar{2}11\bar{3}]$	0.317 4	-0.048 9	0.066 9	0.002 9
4	$(\bar{1}2\bar{1}2)[\bar{1}2\bar{1}\bar{3}]$	0.223 9	-0.012 9	0.024 8	0.008 2
5	$(\bar{1}\bar{1}22)[\bar{1}\bar{1}2\bar{3}]$	0.194 1	0.021 4	0.074 2	0.064 0
6	$(1\bar{2}12)[1\bar{2}1\bar{3}]$	0.140 4	-0.027 7	0.006 3	0.087 1

3 Conclusions

1) The stress and strain tend to be inhomogeneous in polycrystals because the interaction between deformed grains with different orientations, resulting in local plastic deformation, and thereby causing strain and stress heterogeneity within grains.

2) The RS model can predict the formation of slips that is confirmed by experiment.

3) Compared to the deformation behavior of isolated single grain, distinctively different plastic deformation behavior can be observed in the grain surrounded by other grains. Unlike a single grain, additional local slips are initiated to reduce the strain inconsistency among the system.

4) The activation of twinning system depends on the Schmid factor and incompatibility between the deformed grain and its surrounding matrix induced by the twinning. Both slip and mechanical twinning mechanisms should be considered and their combined effects are critical to comprehensively understand the stress and strain consistency during deformation.

References

- 1 Partridge P G. *Metallurgical Reviews*[J], 1967,12(1): 169
- 2 Yoo M H. *Metallurgical and Materials Transactions A*[J], 1981, 12(3): 409
- 3 Sun Qiaoyan, Zhu Ruihua, Liu Cuiping et al. *The Chinese Journal of Nonferrous Metals*[J], 2006, 16(4): 592 (in Chinese)
- 4 Lütjering G, Williams J C. *Titanium*[M]. Berlin: Springer-Verlag Press, 2003
- 5 Liu Yanping, Zhang Hui, Zhang Wangfeng et al. *Rare Metal Materials and Engineering*[J], 2013, 42(6): 1169 (in Chinese)
- 6 Van Houtte P, Li S Y, Seefeldt M et al. *International Journal of Plasticity* [J], 2005, 21(3): 589
- 7 Xie Q G, Van Bael A, Sidor J J et al. *Acta Materialia*[J], 2014,

- 69(5): 175
- 8 Crumbach M, Goerdeler M, Gottstein G. *Acta Materialia*[J], 2006, 54(12): 3275
- 9 Mu S, Tang F, Gottstein G. *Acta Materialia*[J], 2014, 68(15): 310
- 10 Lebensohn R A, Tomé C N, Castañeda P P. *Philosophical Magazine*[J], 2007, 87(28): 4287
- 11 Zhang Xing, Wang Qiang, Zhang Ning et al. *Rare Metal Materials and Engineering*[J], 2019,48(12): 3895 (in Chinese)
- 12 Mao W M. *Frontiers of Materials Science*[J], 2018, 12(3): 322
- 13 Mao W M. *Materials Science and Engineering A*[J], 2016, 672: 129
- 14 Zhang N, Mao W M. *International Journal of Refractory Metals and Hard Materials*[J], 2019, 80: 210
- 15 Kanjarla A K, Van Houtte P, Delannay L. *International Journal of Plasticity*[J], 2010, 26(8): 1220
- 16 Sachs G. *Zeitschrift des Vereines Deutscher Ingenieure*[J], 1928, 72: 732
- 17 Barkia B, Doquet V, Couzinié J P et al. *Materials Science and Engineering A*[J], 2015, 636: 91

冷轧HCP结构合金(CP-Ti)中变形晶粒的晶体学行为: 反应应力模型的实验与模拟

张 宁¹, 孟 利¹, 张 杏², 张文康³, 钟 声⁴, 毛卫民²

(1. 钢铁研究总院有限公司 冶金工艺研究所, 北京 100081)

(2. 北京科技大学 材料科学与工程学院, 北京 100083)

(3. 山西太钢不锈钢股份有限公司, 山西 太原 030003)

(4. ABB美国研发中心, 美国 北卡罗来纳州 27606)

摘 要: 对商业纯钛 (CP-Ti) 退火后冷轧9%变形的板材, 利用电子背散射衍射 (EBSD) 和扫描电子显微镜 (SEM) 评估了晶粒中激活的滑移系统和孪生系统。同时, 采用反应应力 (RS) 模型模拟了变形晶粒中滑移系统的激活以及晶粒之间的相互作用, 该模型将晶粒塑性变形过程视为外加应力和统计变化的晶间反应应力共同作用的结果。结果表明, 反应应力模型适用于评价多晶钛的变形行为。该模型预测了变形后的钛晶粒内发生的滑移, 实验数据证实了该模型的正确性。变形晶粒中滑移和孪晶的分布不均匀, 与晶粒应变分布不均匀相对应。这种不均匀的晶粒应变也可以由取向不同的相邻晶粒变形而产生。当一个晶粒的塑性变形与其相邻晶粒的塑性变形有显著差异时, 就会触发附加的局部滑移, 从而降低晶粒间的应变不协调。塑性应变在某些情况下是通过机械孪生来实现的, 它与滑移协同以满足晶内和晶间的应变连续性。

关键词: 钛; 滑移; 孪生; 模拟; 反应应力 (RS) 模型; 非均匀应变分布

作者简介: 张 宁, 女, 1982年生, 博士, 高级工程师, 钢铁研究总院有限公司冶金工艺研究所, 北京 100081, 电话: 010-62187014, E-mail: zhangning@cisri.com.cn